CONF-790815--19

VAPOR LOCKING AND HEAT TRANSFER UNDER TRANSIENT AND STEADY STATE CONDITIONS

MASTER

by

C.-J. Chen, S.-T. Wang, and J. W. Dawson

Prepared for

International Cryogenic Materials Conference

Madison, Wisconsin

August 21-24, 1979

U of C-AUA-USDOE

ARGONNE NATIONAL LABORATORY, ARGONNE, ILLINOIS

Operated under Contract W-31-109-Eng-38 for the

U. S. DEPARTMENT OF ENERGY

VAPOR LOCKING AND HEAT TRANSFER
UNDER TRANSIENT AND STEADY STATE
CONDITIONS*

C.-J. Chen, S.-T. Wang, and J. W. Dawson

Argonne National Laboratory
9700 South Cass Avenue
Argonne, IL 60439

INTRODUCTION

The technology of stable superconducting magnets has become synonymous with the study and use of composite conductors. The composite conductor, a superconductor paralleled with a normal metal, helps provide magnet stability by supplying alternate electrical and thermal paths for the superconductor when it become normal. If these alternate paths of normal metal can carry the total transport current continuously and still remain below the superconductor transition-temperature, the composite conductor is said to be cryostable. The operational definition of cryostability requires sufficient cooling to dissipate Joule heating.

The degree of cryogenic stability depends on the heat transfer characteristics of the liquid helium cooling channels. Normal zones created following mechanical disturbances will either grow or collapse depending on the heat transfer rates from the conductor to the adjacent cooling channels. It is important to design large magnets with cooling channels sufficiently large so that vapor binding would not occur under both steady state and transient conditions.

Steady state and transient heat transfer to liquid helium channels has been studied by various investigators[1-5]. This study is undertaken to determine the vapor locking in the cooling channels of a cryostable superconducting magnet[6], to investigate the heat transfer characteristics under

*Supported by the U.S. Department of Energy.

steady state and transient conditions, and to study the effects of vapor accumulation of the multiple coil layers.

APPARATUS AND MEASURING TECHNIQUES

To obtain the effects of transient and steady state heat transfer and vapor formation on cryostable conductors, samples are made to simulate the real cryostable superconductor and the cooling channels to be used in the large MHD superconducting magnet called CFFF-SCMS[6]. Which is currently under construction at Argonne National Laboratory (ANL). The cross-section of conductor is 3.1 cm by 0.47 cm and that of cooling channel is 0.97cm by 0.076cm. Figure 1 shows an assembly of simulated single coil-layer. Three conductors are sandwiched with insulation. Those conductors are insulated by 0.064 cm thick pultruded fiberglass strip. A 0.0064 cm thick double-coated adhesive mylar tape is used to bond the conductor together. Therefore, the assembly provides a really cooling channels. This assembly is about 50% covered by 0.64 cm thick G-10 strips so that it simulates an identical cooling conditions to the conductors within the CFFF-SCMS coil structures.

A 0.0025 cm thick stainless steel heater is buried in the middle conductor. The insulation between heater and conductor is 0.0025 cm thick lens paper absorbed with the GE-7031 insulating varnish. The maximum dissipated power of the heater is about 5 kW.

The temperature of conductors is measured using chromel vs. gold-0.07 at% iron thermocouple. The thermocouple insulation has good thermal coupling and is provided by wrapping the indium solder tip of the thermocouple with a single layer of 0.0025 cm thick lens paper absorbed with the GE-7031 varnish.

One can investigate the vapor fraction by means of the change of capacitance in the channel, because the dielectric constant of liquid helium is different from that of gas helium. The capacitance change, ΔC, of channel due to the presence of vapor is given by:

$$\Delta C = C_L \cdot \left(1 - \frac{\varepsilon_L}{\varepsilon_G}\right) \cdot \alpha \quad (1)$$

where α is the volume fraction of helium vapor inside the channel, and C_L is the capacitance of channel when it is filled with 100% liquid helium. When the channel is completely filled with helium gas, the vapor fraction, α, equals to 1, and the capacitance change, ΔC, reaches a maximum value called ΔC_{max}. If the temperature of helium vapor remains constant, Eq. 1 can be simplied as

$$\alpha = \frac{\Delta_C}{\Delta C_{max}} \quad (2)$$

A capacitance bridge with a triaxial cable to compensate for any leakage current is used. The sensitivity of this bridge is about 3 volts per pica-farad capacitance change.

The maximum capacitance change of cooling channel of simulated assembly is about 1.4 pica-farad. The wetted area of front side of middle conductor is 33.98 cm^2 and that of rear side is 16.16 cm^2. The volume of conductor is 28.53 cm^3 and the volume of each channel is 2.58 cm^3.

RESULTS

The experiment was conducted employing either a steady state or transient current to the heater. In either case the temperature difference and the capacitance changes were measured. The capacitance bridge is calibrated before each run. Enough waiting time is allowed after each pulse to ensure the escape of all vapor bubbles from the channels and the cooldown of the conductors to liquid helium temperature.

The terms of heat flux, energy density, temperature rise, and vapor fraction, in the following figures and paragraphs are defined as follows:

heat flux = electrical power to heater/cooling surface area of the conductor;

energy density = electrical energy to heater/conductor volume;

temperature rise = the temperature difference above the temperature of liquid helium;

vapor fraction = volume fraction of vapor in the cooling channel.

Steady State Results

The steady state heat transfer characteristics is shown in Fig. 2. It can be seen from this figure that the critical heat flux for the transition from nucleate boiling to film boiling is about 0.4 w/cm^2 and the recovery heat flux for the transition from film boiling to nucleate boiling is about 0.25 w/cm^2. The temperature rise suddenly change from 0.2 K to about 7 K when the transition of nucleate boiling to film boiling occurs. During the recovery process, the temperature drop suddenly from 1K to 0.1 K soon as it reaches boiling regime. This clearly indicates that single-layer assembly can handle the steady state heat flux up to 0.4 w/cm^2, which means the conductor can dissipate the steady state Joule heating up to 1.16 watts per cm length of conductor. The steady state heat transfer coefficient, h, decreases soon after the peak nucleate heat flux is reached. Therefore, the heat flux transferring to channels decreases.

Figure 3 shows the vapor fraction of front and rear channels versus heat flux. The vapor fraction is about 0.44 for front channel and about 0.36 for rear channel when the heat flux is near peak nucleate heat flux. This is equivalent to about 0.1 cm^3 of liquid helium vaporized within the channels per cm length of conductor.

Transient Results

The pulse duration and power level of heater can be varied to desired values. The vapor fraction and temperature rise presented are the maximum value observed for each pulse. The heat transfer characteristics are presented as following:

Figure 4 shows the energy density versus temperature rise for different pulse durations. It indicates that the temperature rise is function of energy density and is regardless of its pulse duration. The critical energy density for boiling transition is about 100 mJ/cm^3. If the mechanical disturbance dissipate an amount of energy less than the critical value, the peak temperature rise is less than 1 K. When the injected energy density was increased to about 1 J/cm^3, the temperature of conductor rose to about 15 K peak value. The temperature recovery rate is about 0.02 K per milli-second.

Figure 5 shows the heat flux under different pulse duration versus temperature rise. We found that the shorter the pulse duration is, the higher the critical value for boiling transition. When the pulse duration is longer than 200 ms, the heat transfer characteristics approach to that under steady state condition. It can be seen that the critical heat flux for 10 ms pulse is about ten times of the critical heat flux for 200 ms pulse.

The vapor fractions of front channel and rear channel versus heat fluxes for different pulse duration are plotted in Fig. 6. The vapor fraction of front channel is less than that of rear channel at lower heat flux range, but this trend reverse as the heat flux is increased. However, the vapor fraction of front channel is less than that of rear channel again when the heat flux is high enough for the transition of nucleate boiling to film boiling. To explain these phenomena, let's consider following arguments:

(a) At the low heat flux range, both channels are in the free convection regime. In which fluid moves under the influence of buoyant foreces arising from changes in density. The velocity is zero at the heated surface (no-slip boundary condition), increases rapidly in a thin boundary layer adjancent to the surface, and becomes zero again far from the surface. The wetted surface of front side continues from bottom to top, while the wetted surface of rear side is blocked by turn-to-turn insulation. So that the fluid in rear channel moves harder than that in front channel, therefore the vapor fraction in rear channel is greater than that in front channel.

(b) When the heat flux increases, both channels are in the nucleate boiling regime. The vapor bubbles begin to appear at the heating surface and depart from the surface. Since the wetted area of front side is about twice of that of rear side, the energy transferred into the front channel is more than that transferred into the rear channel. The more the energy transferred, the more the liquid helium is vaporized and the greater is the resulting vapor fraction observed.

(c) In the high heat flux range, the liquid helium of the front channel apparently reaches the film boiling regime while the rear channel does not, so that the heat transfer into the rear channel is more than that into front channel. Therefore, the vapor fraction of rear channel is greater than that of front channel.

Figures 7 and 8 show the vapor fraction of the front channel and rear channel versus energy density. The transition to film boiling occurred in the front channel in the 100 mJ/cm^3 range, but it did not occur in the rear channel up to 1 J/cm^3. This result is consistent with the heat flux data of Fig. 6.

CONCLUSIONS

Based on the experimental results obtained the following conclusions can be made:

(1) the critical steady state heat flux for the transition from nucleate boiling to film boiling is about 0.4 w/cm^2.

(2) the critical transient energy density for the boiling transition is about 100 mJ/cm^3.

(3) the front channel is easier to reach the film boiling regime than rear channel, due to that the wetted area of front side is more than the wetted area of rear side.

(4) no temperature rise greater than 1 K is possible if the heat flux does not exceed the critical heat flux under steady state condition or the energy density does not exceed the critical energy density under transient condition.

REFERENCES

1. M. N. Wilson and Y. Iwasa, "Stability of Superconductors Against Localized Disturbances of Limited Magnitude," Cryogenics, 18: 17 (1978).

2. C. N. Whetstone and R. W. Boom, "Nucleate Cooling Stability for Superconductor-Normal Metal Composite Conductors in Liquid Helium," Adv. Cryo. Eng., 13: 68 (1968).

3. O. Tsukamoto and S. Kobayaski, "Transient Heat Transfer Characteristics of Liquid Helium," J. of Appl. Phys., 46: 1359 (1975).

4. G. B. James, K. G. Lewis, and B. J. Maddock, "Critical Heat Fluxes For Liquid Helium Boiling in Small Channels," Cryogenics, 10: 480 (1970).

5. M. A. Hilal, J. W. Dawson, J. D. Gonczy, L. R. Turner, and S.-T. Wang, "Vapor Formation and Heat Transfer in Liquid Helium Cooling Channels under Transient and Steady State Conditions," IEEE Trans. on Mag.-15: 59, (1979).

6. S.-T. Wang, R. C. Niemann, L. R. Turner, L. Genens, W. Pelczarski, J. Gonczy, J. Hoffman, Y-C. Huang, N. Modjeski and E. Kraft, "A Superconducting Dipole Magnet for the UTSI MHD Facility," IEEE Trans. on Mag.-15: 302 (1979).

FIGURE CAPTION

1. Assembly of simulated single coil-layer for vapor locking and heat transfer experiments.
2. Heat transfer characteristics under steady state condition.
3. The characteristics of vapor formation under steady state condition.
4. Heat transfer characteristics under transient condition for different pulse durations.
5. Temperature rise of conductor with respect to heat flux under transient conditons.
6. Vapor fraction of cooling channels with respect to heat flux under transient condition.
7. The characteristics of vapor formation under transient condition for front channel.
8. The characteristics of vapor formation under transient condition for rear channel.

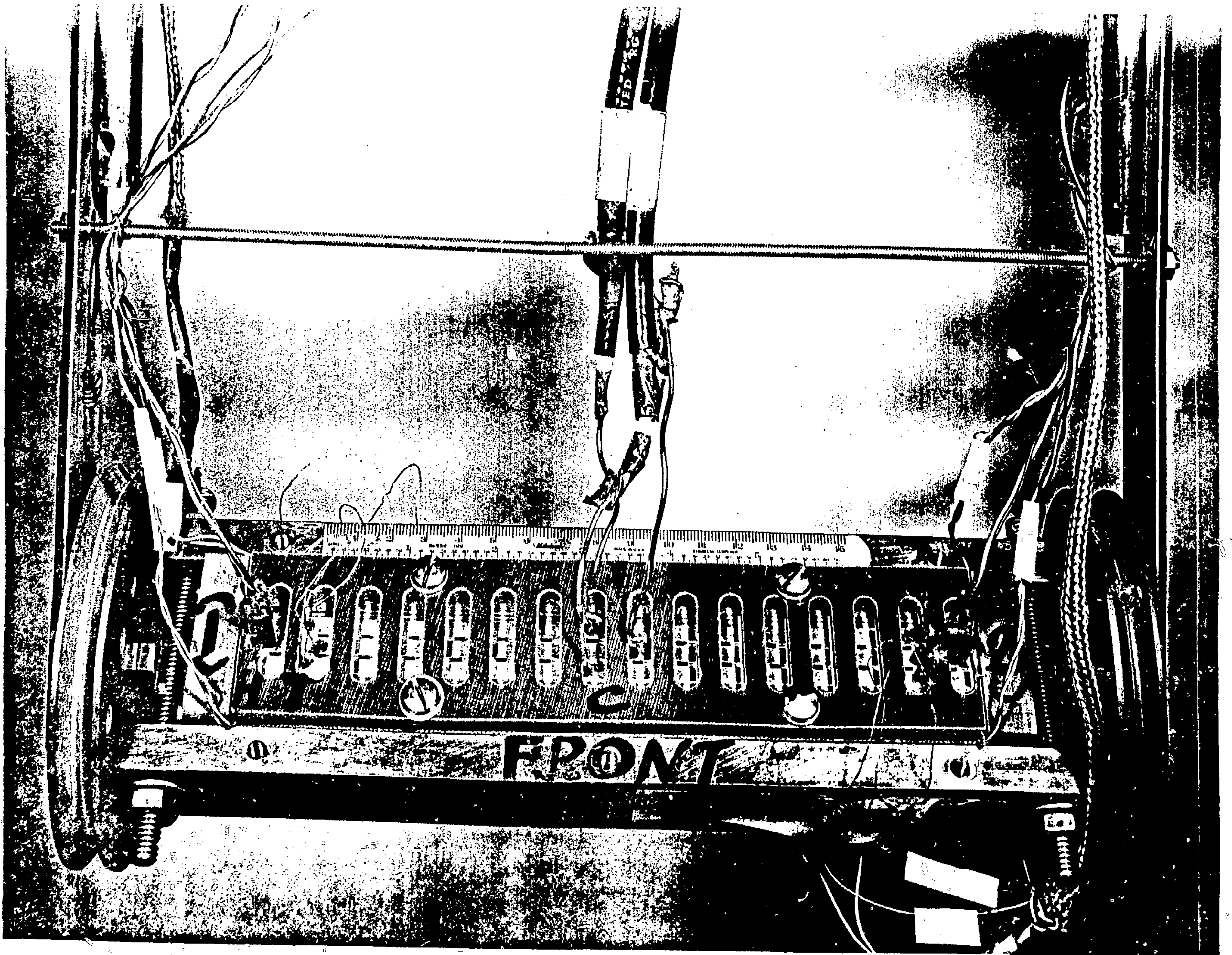
FRONT

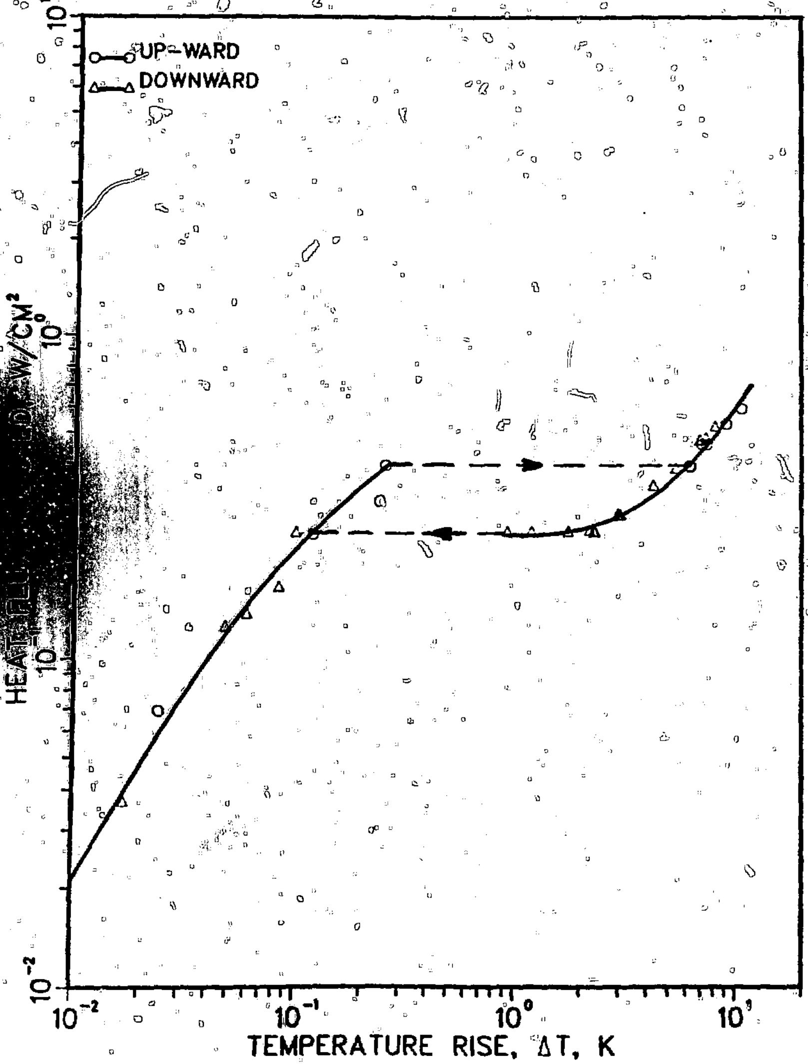
UP-WARD
DOWNWARD
HEAT FLUX, W/CM²
TEMPERATURE RISE, ΔT, K
10⁻²
10⁻¹
10⁰
10¹

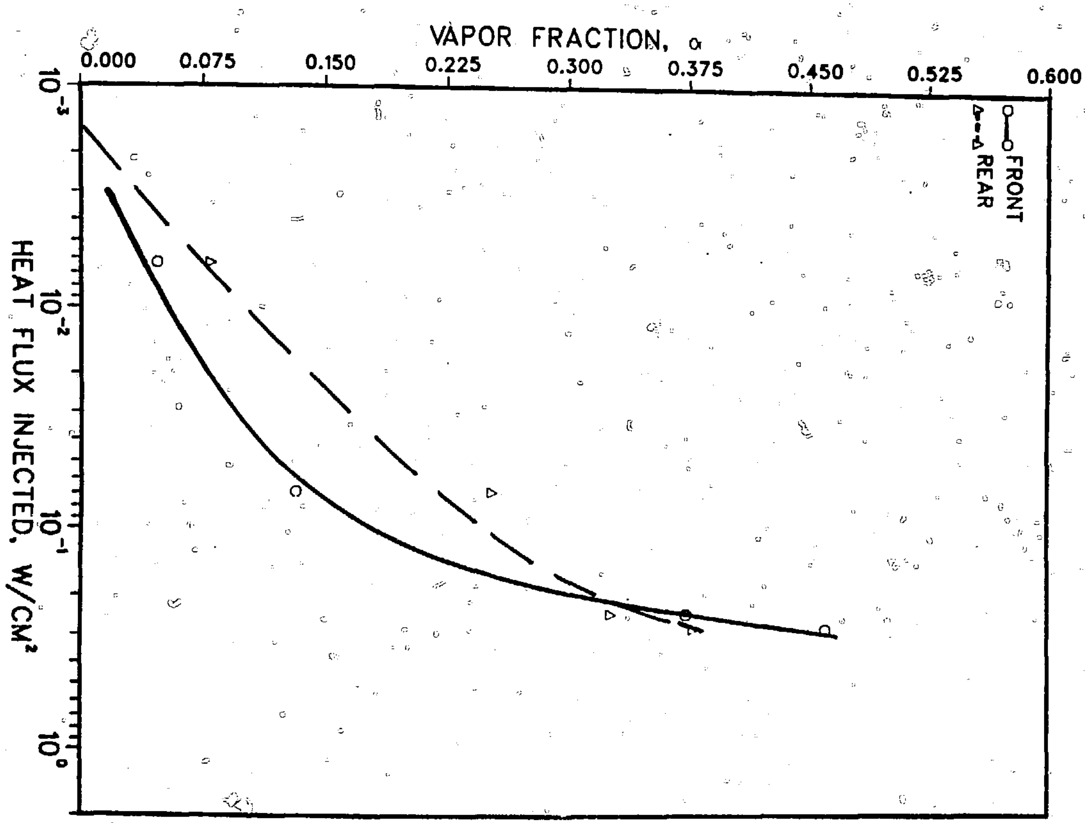
VAPOR FRACTION, α
0.000
0.075
0.150
0.225
0.300
0.375
0.450
0.525
0.600
HEAT FLUX INJECTED, W/CM²
10⁻³
10⁻²
10⁻¹
10⁰
FRONT
REAR

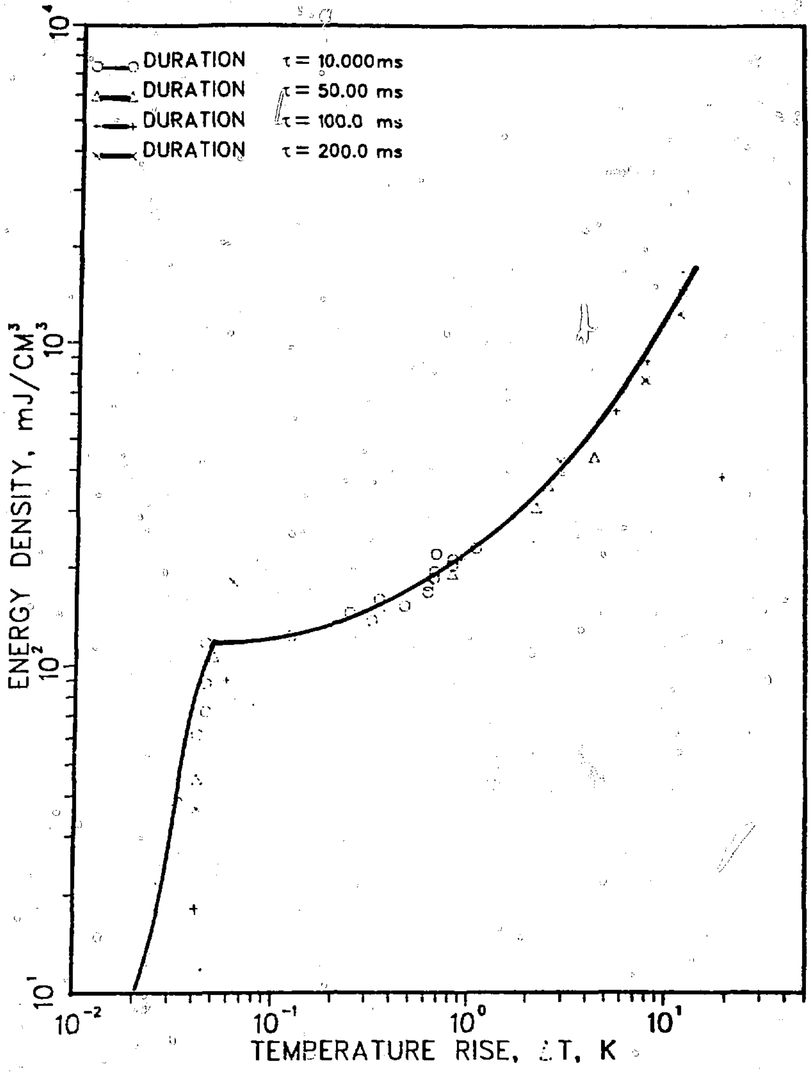

DURATION τ = 10.000 ms
DURATION τ = 50.00 ms
DURATION τ = 100.0 ms
DURATION τ = 200.0 ms
ENERGY DENSITY, mJ/CM³
TEMPERATURE RISE, ΔT, K
10⁴
10³
10²
10¹
10⁻²
10⁻¹
10⁰
10¹

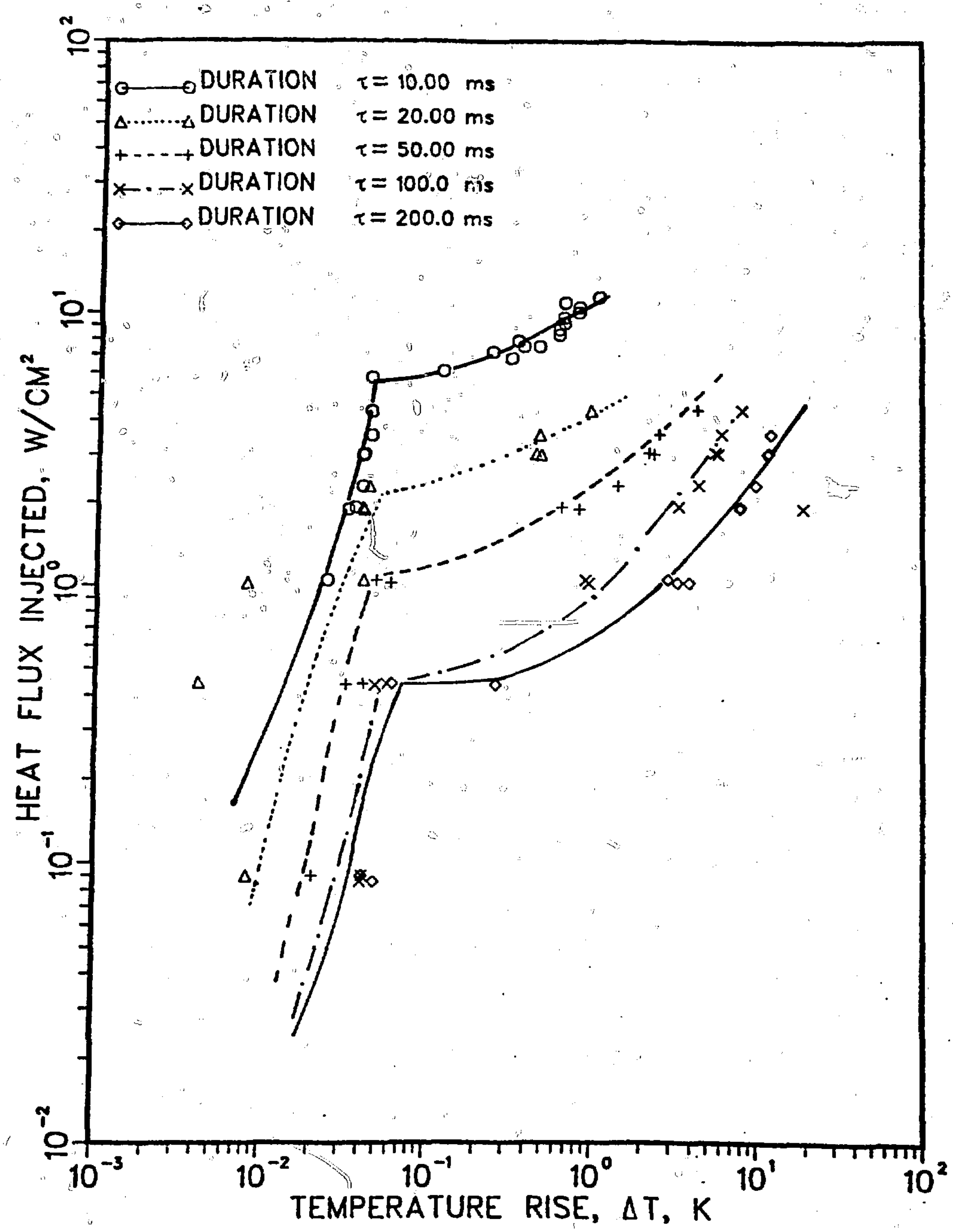

DURATION τ = 10.00 ms
DURATION τ = 20.00 ms
DURATION τ = 50.00 ms
DURATION τ = 100.0 ms
DURATION τ = 200.0 ms
HEAT FLUX INJECTED, W/CM²
TEMPERATURE RISE, ΔT, K
10⁻³
10⁻²
10⁻¹
10⁰
10¹
10²

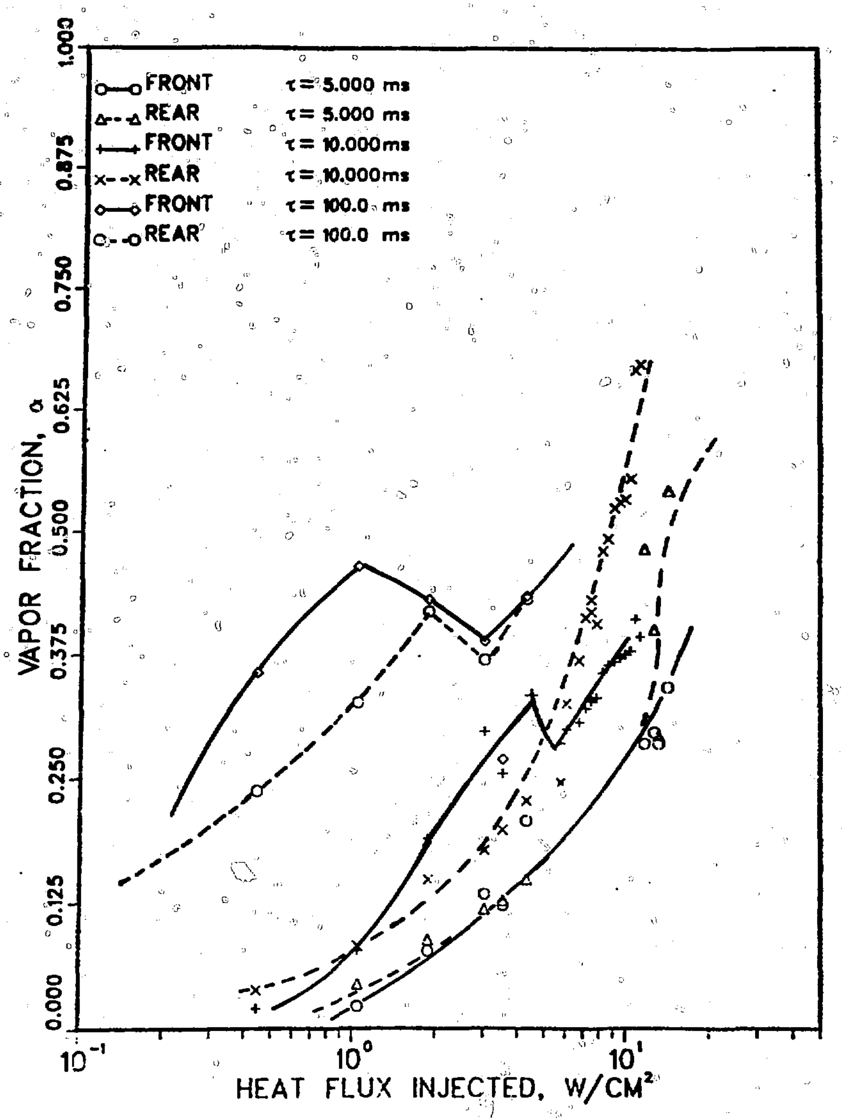
FRONT τ= 5.000 ms
REAR τ= 5.000 ms
FRONT τ= 10.000ms
REAR τ= 10.000ms
FRONT τ= 100.0 ms
REAR τ= 100.0 ms
VAPOR FRACTION, α
0.000
0.125
0.250
0.375
0.500
0.625
0.750
0.875
1.000
10^-1
10^0
10^1
HEAT FLUX INJECTED, W/CM²

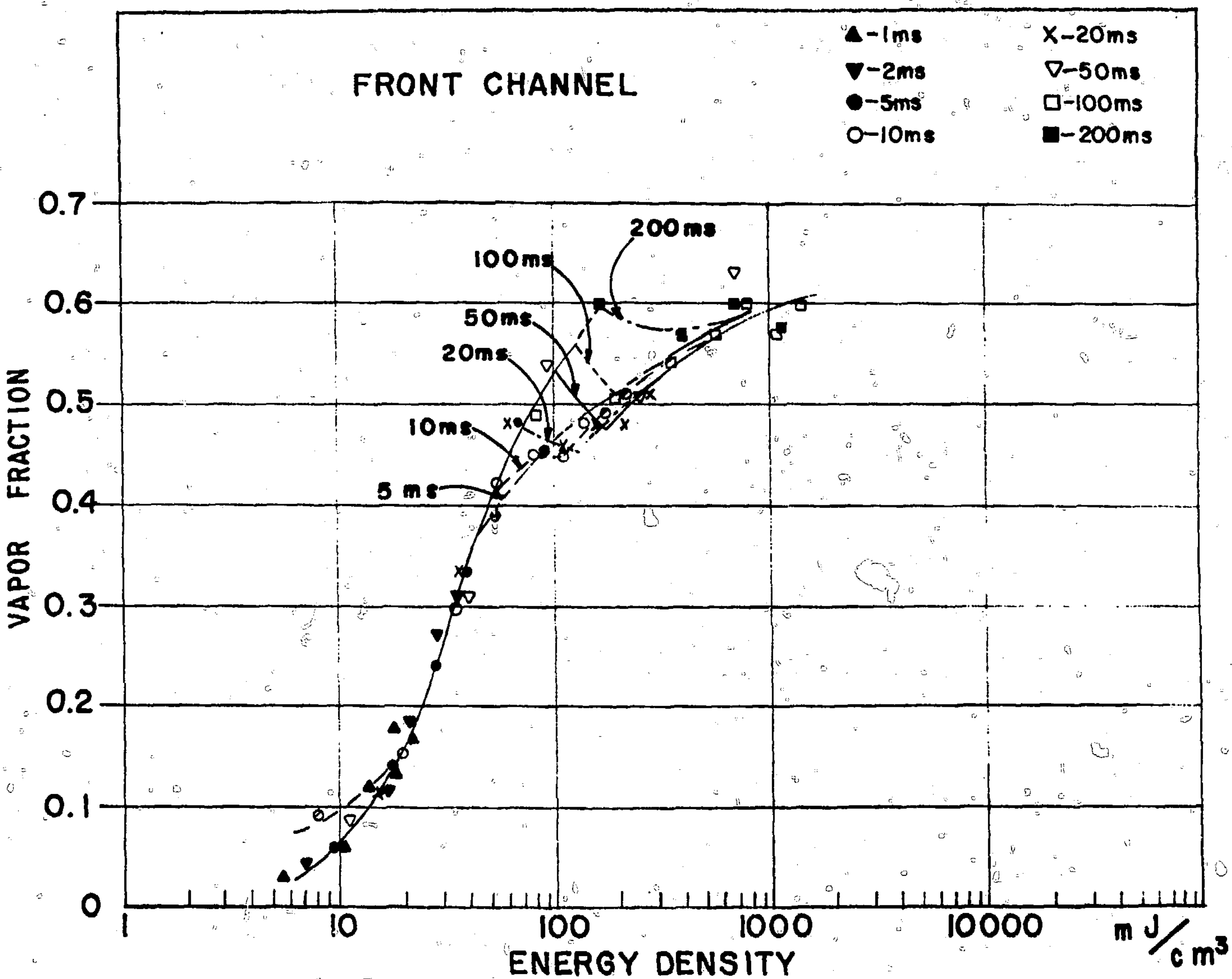

FRONT CHANNEL
▲-1ms
▼-2ms
●-5ms
○-10ms
X-20ms
▽-50ms
□-100ms
■-200ms
200ms
100ms
50ms
20ms
10ms
5 ms
VAPOR FRACTION
0
0.1
0.2
0.3
0.4
0.5
0.6
0.7
1
10
100
1000
10000
mJ/cm3
ENERGY DENSITY

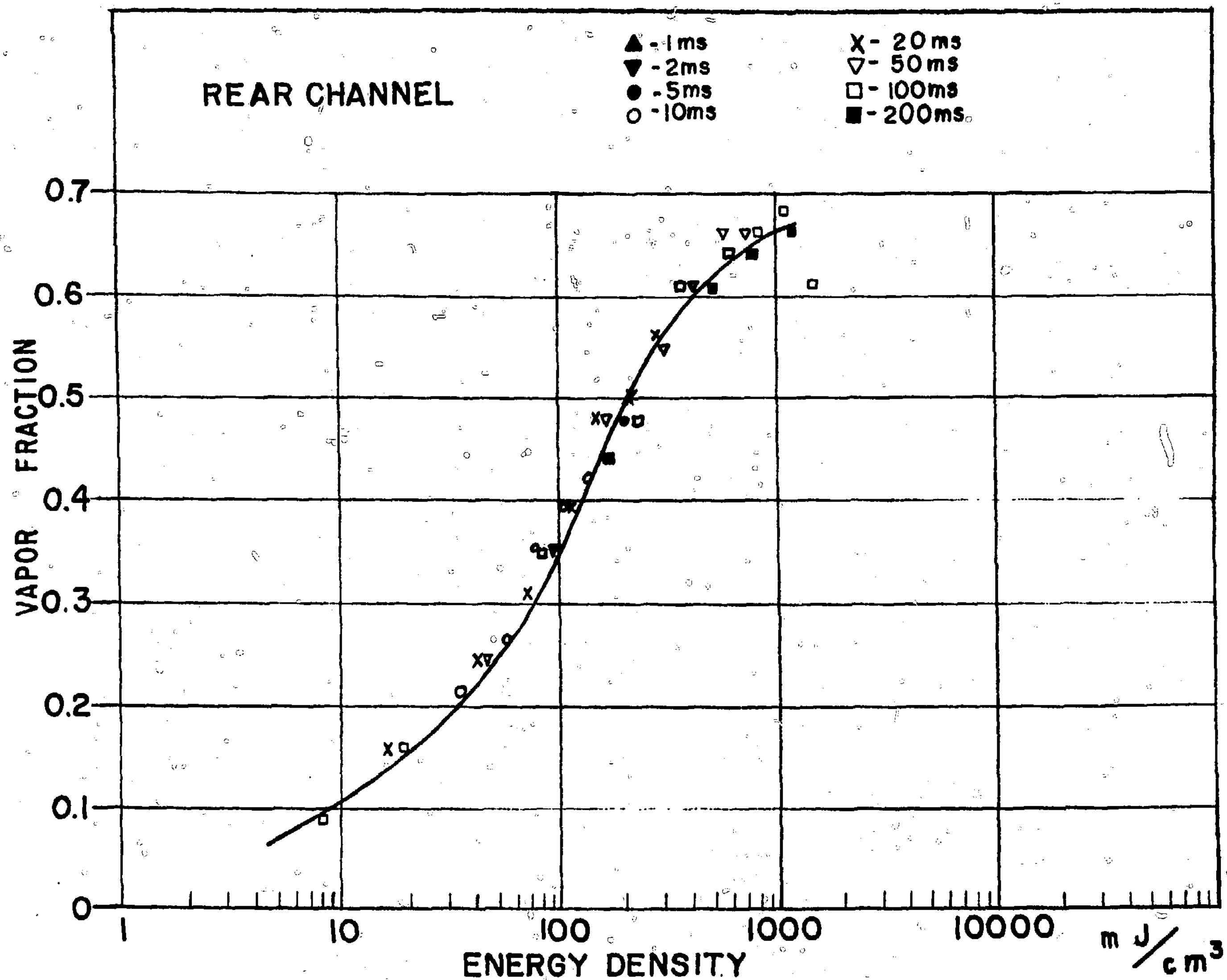
REAR CHANNEL
▲ - 1ms
▼ - 2ms
● - 5ms
○ - 10ms
X - 20ms
▽ - 50ms
□ - 100ms
■ - 200ms
VAPOR FRACTION
0.7
0.6
0.5
0.4
0.3
0.2
0.1
0
1
10
100
1000
10000
mJ/cm3
ENERGY DENSITY